Author's Accepted Manuscript

www.elsevier.com/locate/talanta

Ultra-sensitive "turn-on" detection method for Hg^{2+}based on mispairing biosensor and emulsion PCR

Pengyu Zhu, Wenying Tian, Nan Cheng, Kunlun Huang, Yunbo Luo, Wentao Xu

PII: S0039-9140(16)30265-X
DOI: http://dx.doi.org/10.1016/j.talanta.2016.04.026
Reference: TAL16508

To appear in: *Talanta*

Received date: 3 March 2016
Revised date: 10 April 2016
Accepted date: 11 April 2016

Cite this article as: Pengyu Zhu, Wenying Tian, Nan Cheng, Kunlun Huang Yunbo Luo and Wentao Xu, Ultra-sensitive "turn-on" detection method for Hg^{2+}based on mispairing biosensor and emulsion PCR, *Talanta* http://dx.doi.org/10.1016/j.talanta.2016.04.026

This is a PDF file of an unedited manuscript that has been accepted for publication. As a service to our customers we are providing this early version of the manuscript. The manuscript will undergo copyediting, typesetting, and review of the resulting galley proof before it is published in its final citable form. Please note that during the production process errors may be discovered which could affect the content, and all legal disclaimers that apply to the journal pertain.

ACCEPTED MANUSCRIPT

Ultra-sensitive "turn-on" detection method for Hg^{2+} based on mispairing biosensor and emulsion PCR

Pengyu Zhu[a], Wenying Tian[b], Nan Cheng[a], Kunlun Huang[a,b], Yunbo Luo[a,b], Wentao Xu[a,b*]

[a]Beijing Advanced Innovation Center for Food Nutrition and Human Health, College of Food Science & Nutritional Engineering, China Agricultural University, P.R. China.

[b]Beijing Laboratory for Food Quality and Safety, College of Food Science and Nutritional Engineering, China Agricultural University, Beijing, P. R. China

*To whom correspondence should be addressed.Tel/Fax: +86 010 62736479; Email: xuwentao@cau.edu.cn

Abstract

Sensor-based detection methods have inspired the idea that chemical or physical signals could be converted to nucleic acid signals to be quantitatively detected using a combination of appropriate detection tools. To achieve ultra-sensitive and absolute quantitative detection of mercury ion (Hg^{2+}), we have combined a mispairing biosensor for Hg^{2+} and emulsion PCR. The parameters that might influence the biosensor step, such as the duration of isothermal amplification and the concentration of the sensor oligonucleotide, have been firstly optimized in our study to achieve the most efficient biosensor detection. The evaluation results of secondary structures between the biosensors with different number of T-Hg-T structures achieved by Circular Dichroism have indicated that the secondary hairpin structure would be varied according to the change of number of T-Hg-T structures, which could influence the quantitative detection results. Further optimization of number of T-Hg-T within the biosensor sequences showed that 5 T-Hg-T structures could generate the most efficient amplification. After the above optimizations, the emulsion PCR has been employed to achieve the absolute quantitation of nucleic acid signals. The final results have shown that the limit of quantitation (LOQ) in our study was as low as 40 fmol, and the limit of detection (LOD) was 10 fmol. The practical detection tests showed

Accepted manuscript

ACCEPTED MANUSCRIPT

that the quantitative results were stable and accurate for all substrates. In conclusion, by combining a mispairing biosensor with emulsion PCR, we developed a flexible and stable quantitative "turn-on" detection method with ultra-sensitivity that can detect trace amounts Hg^{2+} within different substrates.

Keywords: Mispairing biosensor; Emulsion PCR; Absolute quantitation; Hg^{2+}

1. Introduction

Of all the heavy metals that are soluble in water, Hg^{2+} is regarded as one of the greatest risks to the human body [1]. Even at very low concentrations, Hg^{2+} solutions can cause brain damage, kidney failure and various disorders of motion and cognition [2]. Therefore, various detection methodologies have been developed to detect trace amounts of mercury ions. Traditional detection methods such as atomic absorption spectroscopy, electron capture devices, inductively coupled plasma optical emission and mass spectrometry with or without chromatographic techniques all require complicated facilities or expensive and time-consuming sample preparation [3–5]. Recently, the detection methods based on biosensors have been developed rapidly due to their relative simplicity and low cost [6–8]. Most sensors are based on the conversion of chemical or physical signals to nucleic signals[9,10]. Thus, this transmission has provided a thought that the detection of the Hg^{2+} could be instead by the detection of the nucleic signal [6,8,11–14]. There are two main types of biosensor-based detection methods: "turn-on" biosensors and "turn-off" biosensors [15,16]. For "turn-off" sensors, the cleavage of the substrate sequence usually decreases the original nucleic acid signal. However, "turn-off" sensors are mostly not suitable for analytical proposes. First, the decrease of the targeted signals is usually 1-fold. This indicates that changes in lower signals could not be accurately captured. Second, "turn-off" sensors can be easily influenced by quencher groups in natural samples, causing false positive or false negative results. Recently, a type of "turn-on" biosensor

Accepted manuscript

ACCEPTED MANUSCRIPT

for the specific detection of Hg^{2+} based on the mispairing of thymine-Hg^{2+}-thymine (T-Hg-T) has been developed to achieve the sensitive and selective detection of Hg^{2+} [6–8,11–14,17–21]. With this "turn-on" biosensor, the signal of Hg^{2+} can be converted to a nucleic acid signal with a quantitative relationship, which is the key to achieve quantitative detection. Different studies have used this type of biosensor by combining different nucleic acid signal detection methods, including fluorescent detection[22], isothermal amplification [17], hemin/G-quadruplex DNAzyme structure [19], microarray chips [21], electrochemical[23,24] and carbon dots or graphene [20]. All of the above methodologies have achieved relatively sensitive detection of Hg^{2+}. However, for amplification or optical methods, the side effects caused by PCR[25–27] or fluorescence inhibitors[28–30] cannot be easily avoided, which can cause the unspecific amplification or the change of fluorescence emission. Moreover, for the aforementioned methods, standard curves are always used as part of the quantitative measurements, and this introduces complications in the calculations.

To achieve the absolute quantitative detection of the Hg^{2+} ion, two key elements are required. First, there must be linear signal conversion from the non-nucleic acid signal to the nucleic acid signal. Because Hg^{2+} biosensors based on the specific structure of T-Hg-T have a specific binding model between the biosensor and Hg^{2+}, the signal conversion would follow a certain pattern. Second, nucleic acid signal detection methods should achieve absolute quantitative detection. For normal PCR-based technologies, such as real-time PCR or isothermal amplification methods, quantitative detection is always based on standard curves.

Emulsion PCR is regarded as an improved version of original PCR. It uses a large number of droplets to separate the reaction into many small volumes [31–36]. By separating the original amplification volume and producing a W/O (water-in-oil) structure, this method balances amplification efficiency with the avoidance of substrate effects caused by the PCR tubes [33]. Thus, emulsion PCR is more suitable for the amplification of samples with low-abundance targets or complex

Accepted manuscript

ACCEPTED MANUSCRIPT

substrates[37]. Moreover, because of the generation of a W/O structure, the amplification mixture and templates are also divided. The distribution of materials follows a Poisson distribution [38]. By combining a flow instrument with fluorescence detection, the fluorescence of each droplet can be detected. After the droplet reading step, positive and negative droplets can be recognized in a final heatmap. The copy number of the target sequence can be calculated using the Poisson distribution by considering the ratio of positive and negative droplets. Emulsion PCR has developed rapidly since it was first introduced. Different applications, such as amplification of gene libraries [33,34,39] and single-molecule detection [32,40], have been devised to take advantage of the balanced amplification efficiency of the droplets. Because the division of targets follows the Poisson distribution, quantitative detection can be achieved using fluorescence detection in flow instruments. This quantitative detection method can be regarded as an important alternative way to the quantify targets by real-time PCR with standard curves.

Considering the demand for quantitative detection of Hg^{2+}, we have achieved the absolute quantitative detection of Hg^{2+} by combining a mispairing biosensor and emulsion PCR. Our detection system has the advantages of "turn-on" signal transmission in the sensor step and absolute quantitation by emulsion PCR combined with flow fluorescence detection instruments. According to the results of our study, the limit of quantitation of our detection system is 40 fmol, which was determined by evaluating different samples in parallel. The limit of detection (LOD) was 10 fmol, which was regarded as the lowest Hg^{2+} concentration that could be differentiated from the negative group.

2. Materials and methods

2.1. Oligonucleotides and reagents

The sequences of all oligonucleotides and probes are listed in Table S1. All primers

Accepted manuscript

ACCEPTED MANUSCRIPT

and probes were synthesized by Invitrogen (Life Technologies, CA, US). The chemical reagents used in our study, including the standard $Hg(NO_3)_2$ solution, were purchased from Sigma-Aldrich (St. Louis, MO, USA). All reagents related to the emulsion PCR were purchased from Bio-Rad (Pleasanton, CA, USA).

2.2. Preparation of practical detection sample

For the evaluation of practical samples in our study, polluted water and serum were used as test materials. The water was collected directly from a populated area of Beijing, China. The serum samples were collected by centrifuging mouse blood samples at 3000 rpm for 15 min. After samples were collected, different concentrations of Hg^{2+} solutions were added manually. All samples with additional Hg^{2+} were then placed on the Dynamic CM-200 mixer and shaken overnight to achieve an equal distribution.

2.3. Isothermal amplification of biosensor

The isothermal amplification of the biosensor sequence could occur after the formation of a hairpin structure with the synthesis of T-Hg-T mispairings. After the mixing of biosensor oligonucleotides and Hg^{2+}, the temperature of the solution was raised to 95 ºC to achieve complete denaturation. Then, the temperature was slowly reduced to room temperature to generate the T-Hg-T mispairings. The dNTP mixture (Takara, Dalian), as well as the buffer and enzyme for Klenow Fragment (3'→5' exo-), were added to the above mixture to achieve isothermal amplification. The duration of isothermal amplification and final concentration of biosensor oligonucleotides were optimized in our study.

2.4. Emulsion PCR assay

Serial dilutions of the product of the isothermal amplification were performed before the emulsion PCR step to ensure the proper copy number range. The final emulsion

Accepted manuscript

ACCEPTED MANUSCRIPT

PCR volume contained 1× PCR Master Mix (Bio-Rad), reverse and forward primers at a final concentration of 0.24 μmol L^{-1} and a TaqMan probe at a final concentration of 0.12 μmol L^{-1}. The final concentrations of added templates varied for different assays, while the added volume was 2 μL of the total 20 μL volume. The droplets of the reaction volume for emulsion PCR were generated by using a disposable eight-channel droplet generator cartridge (Bio-Rad). The prepared reaction volume was then used for PCR amplification. After thermal cycling, each droplet of the reaction volume was passed through the flow instrument for fluorescence detection (Bio-Rad). The fluorescence of each droplet was measured. For the detection of the fluorescence signal, the FAM group was regarded as the reading target, which has an excitation wavelength of 492 nm and emission wavelength at 518 nm.

The PCR amplification procedure consisted of pre-denaturation at 95℃ for 5 min, 50 cycles of two-step thermal cycling involving 10 s at 95℃ for denaturation and 60 s at 60 °C.

2.5. Real-time PCR assay

The real-time PCR assay in our study was performed by the Bio-Rad C1000 PCR facility. The reaction volume of the real-time PCR was as same as the emulsion PCR. The fluorescence of each tube was collected automatically to generate amplification curves. The results were analyzed according to the standard or amplification curves.

2.6. Secondary structure determined by circular dichroism (CD)

The Chirascan™-plus CD Spectrometer (Applied Photophysics, UK) was used to collect CD measurements in our study. To compare the different secondary structures produced by different T-Hg-T sites within the biosensor sequence, CD measurements were used to evaluate the differences between the secondary structures. A total 200 μL reaction volume was collected for these measurements. The final concentration of DNA was suggested to be at least 10 μmol L^{-1} according to the official guidelines. For

Accepted manuscript

ACCEPTED MANUSCRIPT

the final 200 μL volume, 10 μmol L^{-1} of biosensor oligonucleotide was included, as well as 1×isothermal amplification buffer and the appropriate concentration of Hg^{2+} to form the complete hairpin structure.

2.7. Data analysis

The absolute copy number of the volume of emulsion PCR was determined based on the ratio of positive droplets to total droplets. The copy number of target sequence was calculated according to the Poisson distribution:

$$A(samples) = -ln[(N - X)/N] \times N \ldots\ldots\ldots (1)$$

For the above equation, A (samples) was defined as the absolute copy number of the target sequence in the emulsion PCR reaction volume. N and X were defined as the total and positive droplets of each reaction volume, respectively.

For the convenience of data analysis in our study, we have manually defined a parameter, the Elongation Rate (ER), that can be used to evaluate the biosensor elongation step. In our study, the ER was calculated as follows:

$$ER(sample) = \frac{n}{4816} \times A(sample) \ldots\ldots\ldots (2)$$

A (sample) defined as in equation (1). The variable n is defined as the number of T-Hg-T structures within the biosensor sequence. The number 4816 is based on the combination of the serial dilutions and the Avogadro constant.

3. Results

3.1. Principle of our detection system

A diagram of our detection system is shown in Figure 1. It has three main steps: the isothermal sensor elongation step, the emulsion PCR step and the droplet reading step. For the first step, the signal of Hg^{2+} was converted to nucleic acid signal with linear relationship within a certain range. As the structure of T-Hg-T was reported to be

Accepted manuscript

ACCEPTED MANUSCRIPT

stable at lower temperature, we have chosen the Klenow Fragment (3'→5' exo-) as the isothermal amplification enzyme in our study, which has the best enzyme activity at 37℃. The T-Hg-T structure was generated after denaturation and slowly cooling to 37℃. Then, the isothermal enzyme was used to generate blunt ends. During the emulsion PCR step, droplets containing positive or negative sequences were generated. During the droplet reading step, only the droplets containing blunt terminal sequences could generate positive signals. The final heatmap was generated based on the analysis of each droplet. A unique threshold was set to largely distinguish the negative and positive droplets. The absolute copy number of the target sequence could be calculated using the ratio of positive droplets to total droplets according to the Poisson distribution.

3.2. Different secondary structures caused by the number of T-Hg-T structures

The biosensor step in our study depends on the formation of hairpin structures within the biosensor sequence, which interact with Hg^{2+} by generating T-Hg-T mispairing structures. In theory, biosensors with different numbers of T-Hg-T structures would generate different hairpin structures that might have effect on the quantitative measurements. To make sure that the effects on absolute quantitative detection were caused by different hairpin structures within the biosensor, we evaluated different secondary structures of the biosensor with various T-Hg-T structures using CD measurements. According to the CD measurements (Figure 2), different characteristic peaks in the final curves indicate that the biosensors with different numbers of T-Hg-T structures produce various different secondary structures. Therefore, the absolute quantitative detection in our study would be influenced by the T-Hg-T structures within the sequence of the biosensor through the signal transmission of T-Hg-T mispairing. For later experiments, the effects caused by the number of T-Hg-T structures were evaluated to achieve better quantitation.

Accepted manuscript

ACCEPTED MANUSCRIPT

3.3. Effect of the number of T-Hg-T structures

The Hg^{2+} detection system described in our study was based the specific structure of T-Hg-T, which is regarded as a more stable type of binding compared with normal A-T. The number of T-Hg-T structures within the biosensor would be expected to affect the annealing step between the biosensor and the primers of the emulsion PCR. On the other hand, different number of T-Hg-T could affect signal transmission of the biosensor step by directly causing different transfer ratios between the non-nucleic acid signal and the nucleic acid signal. According to our results, for the group that contained 2 T-Hg-T structures, extremely low amplification signal was detected, possibly because it was impossible to form a complete hairpin structure. Thus, elongation of the biosensor sequence could not take place. We also examined sequences containing 5 and 7 T-Hg-T structures. To make appropriate judgments about the differences between the sequences, we examined the amplification signals of groups of serially diluted Hg^{2+} samples. The amplification curves for these groups are shown in Figure S1. The results show that the biosensor with 5 T-Hg-T structures had better dynamic range than the biosensor with 7 T-Hg-Ts. Therefore, in our study, to achieve better amplification of signal and a larger dynamic range, the biosensor containing 5 T-Hg-T structures was used for further testing.

3.4. Optimization of biosensor step

The biosensor step in our study was based on elongation using an isothermal amplification enzyme. Thus, the factors that potentially effect the isothermal amplification could also have side effects in our detection system. In our study, the final concentration of biosensor oligonucleotide and the elongation duration were optimized to achieve better performance. The evaluation results for elongation duration showed that longer elongation times had positive effects on the final biosensor performance. However, little difference was observed when the elongation

Accepted manuscript

ACCEPTED MANUSCRIPT

time was raised above 2 h (Figure S2). Thus, to simplify our detection system, the elongation time was set to 2 h. Additionally, based on our tests of different final concentrations of the biosensor sequence, we found that adding more biosensor sequences had a positive effect on the final signal amplification. However, we also found that the signal increased very little when the final concentration of the biosensor was raised above 0.6 μmol L^{-1}. Therefore, the optimized final concentration of the biosensor sequence was set to 0.6 μmol L^{-1}.

3.5. Quantitative measurement

Based on the experiments described in the previous sections, absolute quantitation could be achieved by combining biosensor and flow reader instruments. For the biosensor step in our detection system, the ion signal could be transferred to the nucleic acid signal within a certain range of Hg^{2+} concentrations. This range was regarded as the dynamic range in our study because Hg^{2+} concentrations could be stably quantified. To determine the dynamic range of our study, we have examined serial dilutions of the original Hg^{2+} solution with a wide range of concentrations, which varied from 0.1 mol L^{-1} to 0.01 pmol L^{-1}. The amplification heatmaps of different groups were listed in the Figure S3. The scatter diagram and standard curve describing the relationship between the concentration of Hg^{2+} and the elongation rate were plotted (Figure 3a and 3b). The two figures showed that the detection system in our study could achieve stable quantitation within a wide dynamic range, from 40 pmol to 40 fmol. The wide dynamic range, which covered over 4 logarithms, indicated that our detection system based on mispairing biosensor and emulsion PCR could meet the quantitative needs of all types of practical samples.

The limit of quantitation (LOQ) in our study was defined as the lowest concentration of Hg^{2+} that could be stably quantified. The LOQ value was determined by analyzing the scatter plot and the standard curve describing the relationship between the ER and the concentration of Hg^{2+}. As shown in the scatter plot (Figure 3b), we found that the

Accepted manuscript

ACCEPTED MANUSCRIPT

relationship between the ER and the concentration of Hg^{2+} was not linear when the concentration of Hg^{2+} was below 40 fmol or above 40 pmol. Therefore, the LOQ in our study was determined to be 40 fmol of Hg^{2+}. This extremely low LOQ suggests that the biosensor detection system used in our study could achieve stable quantitative detection for samples with extremely low Hg^{2+} concentrations.

3.6. Specificity evaluation

In our study, specificity was achieved if no signal was detected when other interfering ions were used as samples. To cover most types of ions, ions with different valences were tested. Ions that are harmful to humans and usually found in labs, such as Ag^{+}, Ni^{2+}, Co^{2+}, Cd^{2+}, Fe^{2+}, Cu^{2+}, Zn^{2+}, Pb^{2+}, Fe^{3+}, and Cr^{6+}, were evaluated in these tests. The final results (Figure 4) showed that other ions could be easily distinguished from positive samples. This indicated that the detection system in our study had a good specificity for Hg^{2+} in the presence of different types of ions.

3.7. Evaluation of interference caused by other ions

Interference caused by other ions was defined as side effects arising from other ions being present in the reaction volume along with the target ion. Specificity was evaluated in the previous section, so we used only Cu^{2+} as a representative interfering factor for these experiments. We kept the final concentration of the target ion constant, and the concentrations of the interfering ion were varied from 100 to 0.5 times that of the target ion. A reaction volume with no interfering ion was set up as positive control. The final concentration of Hg^{2+} was measured by our detection system together with the interfering ion. As shown in the final detection results (Figure S4), the interfering groups showed no significant differences from the positive control group. This indicates that our detection system could specifically detect Hg^{2+} even in the presence of other interfering ions.

Accepted manuscript

ACCEPTED MANUSCRIPT

3.8. Sensitivity determination

The sensitivity of our Hg^{2+} detection system was defined as the lowest concentration that could be stably detected. The sensitivity was evaluated using serial dilutions of the original Hg^{2+} solution. The ER difference between the experimental and negative control group was used to determine the sensitivity in our study. The results are shown in Table 1. As shown in this table, the ER of the 10 fmol group showed obvious differences compared with the negative control group, and the lower group showed little difference. Thus, according to these results and the signal from the negative group, the sensitivity of the detection system was determined to be 10 fmol.

3.9. Evaluation of practical samples

To evaluate the practicality of our detection system, the Hg^{2+} concentrations of different samples, such as natural drinkable water and serum samples, were determined using our Hg^{2+} detection system. As shown in Table 2, our Hg^{2+} detection system showed good stability for different experimental samples. In the collected water samples and serum samples, there was little or no Hg^{2+} present; thus, we added additional Hg^{2+} manually to both types of samples to evaluate the stability of our Hg^{2+} detection system. The final results show that our Hg^{2+} detection system based on a biosensor and emulsion PCR is practical to use for different types of samples.

4. Discussion

An ultra-sensitive absolute Hg^{2+} detection system based on a mispairing biosensor and emulsion PCR has been developed in our study. Taking advantage of the signal transmission of the turn-on mispairing biosensor and the sensitive and quantitative detection of emulsion PCR, we have achieved ultra-sensitive quantitative detection with extremely low LOQ and LOD for the reaction duration within 5 hours.

Accepted manuscript

ACCEPTED MANUSCRIPT

The "turn-on" mispairing Hg^{2+} biosensor was based on the formation of T-Hg-T structures that could generate hairpin structures within the biosensor. In this manner, the target product would increase as the increase of the detection objective, Hg^{2+} in our study. After generation of the hairpin structures, amplification could occur to generate blunt ends within the biosensor sequences. During this step, the generation of the hairpin structure and the ratio of nucleic acid signal transmission were essential to later isothermal amplification. Therefore, the number of T-Hg-T structures affected the final results by influencing the stability of the hairpin structures and the ratio of signal transmission. We evaluated the secondary structures of biosensors with different T-Hg-T structures using CD measurements. The results of the CD measurements showed that biosensors with different numbers of T-Hg-T structures lead to different secondary structures. Moreover, according to the characteristic peaks of different biosensors, we concluded that increasing the number of T-Hg-T structures within the biosensor could cause a red shift in the characteristic peaks. For biosensors with 2, 5, or 7 T-Hg-T structures, the curves of those with 5 or 7 T-Hg-T structures were clearly smoother and higher than the curve of biosensors with 2 T-Hg-T structures. This indicates that the stability of the hairpin structure within the biosensor sequence could be affected by the number of T-Hg-T structures. Hairpins with 2 T-Hg-T structures or fewer would be less stable in the isothermal amplification step. This conclusion, based on CD measurements, could be perfectly proven by the real-time PCR results for the optimization of the number of T-Hg-T structures within the biosensor structure. The number of T-Hg-T structures also had an obvious influence on quantitative detection after the biosensor steps. According to the results achieved using real-time PCR, we concluded that a higher number of T-Hg-T structures could have a side effect on the dynamic range of absolute quantitative detection in our study. A lower number of T-Hg-T structures would have side effects on the formation of hairpin structures, whereas a high number of T-Hg-T structures would adversely affect the dynamic range. Therefore, according to the optimized results in our study, 5

Accepted manuscript

ACCEPTED MANUSCRIPT

T-Hg-T structures was considered to be the optimum amount within the biosensor sequence, which provides the best conditions for both the dynamic range and the formation of hairpin structures.

Emulsion PCR was used to amplify the nucleic acid signal in our study. Compared with traditional amplification, emulsion PCR has many advantages. In traditional amplification methods, the PCR efficiency varies in different locations within the amplification tube. The heterogeneous amplification efficiency causes inaccurate amplification results. Emulsion PCR is more appropriate for measuring low-abundance samples. Because emulsion PCR is based on the generation of extremely small droplets with W/O structure (water-in-oil structure), enhanced tolerance to amplification inhibitors is expected. The separation of the amplification volume reduces the effect of inhibitors compared with traditional amplification. Additionally, emulsion PCR divides the original reaction volume into a large number of droplets. Thus, absolute quantitation can be achieved by counting the positive droplets and negative droplets and making calculations based on the Poisson distribution. This quantitation method represents an improvement compared to traditional real-time amplification. Therefore, by considering the above three parameters, emulsion PCR combined with a flow instrument for fluorescence detection can be regarded as an absolute quantitative detection method in our study. Since the commercialization of emulsion PCR, different platforms have been developed to make the generation of droplets more convenient. Although different platforms use different methods to generate the droplets, the basic principle and the procedures of data analysis are very similar. In our study, droplets were generated with the Bio-Rad platform. This indicates the stability of combining biosensor methods and emulsion PCR. Because the basic principle is similar in all emulsion platforms, we expect that this stability should extend to all emulsion PCR platforms.

According to the final results, the combination of mispairing biosensor and emulsion amplification results in ultra-sensitive absolute quantitative measurement of Hg^{2+}.

Accepted manuscript

ACCEPTED MANUSCRIPT

After the detailed optimization, the LOQ and LOD were set up to 40 fmol and 10 fmol for the content of mercury ion, which regarded as 2 nmol L^{-1} and 0.5nM for the original concentration of mercury solutions. Compared with other detection methods based on biosensor amplification, although the previous could also achieve the detection limit of nmol L^{-1} level, the quantitative limit of most methodologies were lower than the LOQ in our study. Moreover, evaluations of the specificity and the addition of interfering ions indicate that the detection system has a good specificity; it only recognizes the Hg^{2+} signal, even in solutions that have other ions present. Additionally, our testing of environmental and clinical samples indicated that our detection system could meet the practical needs of researchers for the detection of Hg^{2+} in different substrates. In conclusion, according to the results from all the components of our study, we believe that our Hg^{2+} detection system based on a biosensor and emulsion PCR can be regarded as an ultra-sensitive detection method for the measurement of Hg^{2+} in different experimental substrates.

5. Conclusion

The sensor system based on the T-Hg-T structures and emulsion PCR was developed in our study to achieve the absolute quantitation detection of mercury ion. Our sensor system has taken advantage of linear signal conversion of mercury sensor based on T-Hg-T structures and the absolute quantitation of nucleic signal of emulsion PCR. The elements that might have the potential effect to the final results have been detailed optimized, including the numbers of T-Hg-T structures within the sensor oligonucleotide, the duration of isothermal amplification and the final concentration of oligonucleotide in the isothermal amplification volume. Based on the above optimizations, the final results have shown that the LOQ in our study was as low as 40 fmol, and the limit of detection LOD was 10 fmol. The practical detection tests showed that the quantitative results were stable and accurate for all substrates.

Accepted manuscript

ACCEPTED MANUSCRIPT

Therefore, we consider that the sensor system in our study could meet all the demands of the detection of mercury ion within different substrates.

Reference:

[1] B. Patterson, J. Ryan, J.H. Dickey, The toxicology of mercury., N. Engl. J. Med. 350 (2004) 945–947.

[2] T.W. Clarkson, L. Magos, The toxicology of mercury and its chemical compounds., Crit. Rev. Toxicol. 36 (2006) 609–662.

[3] Y. Gao, Z. Shi, Z. Long, P. Wu, C. Zheng, X. Hou, Determination and speciation of mercury in environmental and biological samples by analytical atomic spectrometry, Microchem. J. 103 (2012) 1–14.

[4] Y. Cai, Speciation and analysis of mercury, arsenic, and selenium by atomic fluorescence spectrometry, Trends Anal. Chem. 19 (2000) 62–66.

[5] K. Leopold, M. Foulkes, P. Worsfold, Methods for the determination and speciation of mercury in natural waters-A review, Anal. Chim. Acta. 663 (2010) 127–138.

[6] J. Liu, Y. Lu, Rational Design of "Turn-On" Allosteric DNAzyme Catalytic Beacons for Aqueous Mercury Ions with Ultrahigh Sensitivity and Selectivity, Angew. Chemie. 46 (2007) 7587–7590.

[7] Q. Shen, W. Li, S. Tang, Y. Hu, Z. Nie, Y. Huang, et al., A simple "clickable" biosensor for colorimetric detection of copper(II) ions based on unmodified gold nanoparticles, Biosens. Bioelectron. 41 (2013) 663–668.

[8] X. Zhu, L. Chen, Z. Lin, B. Qiu, G. Chen, A highly sensitive and selective "signal-on" electrochemiluminescent biosensor for mercury., Chem. Commun. 46 (2010) 3149–51.

[9] J. Liu, Z. Cao, Y. Lu, Functional nucleic acid sensors, Chem. Rev. 109 (2009) 1948–1998.

Accepted manuscript

ACCEPTED MANUSCRIPT

[10] S.S. Iqbal, M.W. Mayo, J.G. Bruno, B. V. Bronk, C.A. Batt, J.P. Chambers, A review of molecular recognition technologies for detection of biological threat agents, Biosens. Bioelectron. 15 (2000) 549–578.

[11] N. Kanayama, T. Takarada, M. Maeda, Rapid naked-eye detection of mercury ions based on non-crosslinking aggregation of double-stranded DNA-carrying gold nanoparticles., Chem. Commun. 47 (2011) 2077–9.

[12] M. Li, X. Zhou, W. Ding, S. Guo, N. Wu, Fluorescent aptamer-functionalized graphene oxide biosensor for label-free detection of mercury(II)., Biosens. Bioelectron. 41 (2013) 889–93.

[13] F. Ma, Y. Zhang, H. Qi, Q. Gao, C. Zhang, W. Miao, Ultrasensitive electrogenerated chemiluminescence biosensor for the determination of mercury ion incorporating G4 PAMAM dendrimer and Hg(II)-specific oligonucleotide, Biosens. Bioelectron. 32 (2012) 37–42.

[14] Y. Zhang, H. Zhao, Z. Wu, Y. Xue, X. Zhang, Y. He, et al., A novel graphene-DNA biosensor for selective detection of mercury ions, Biosens. Bioelectron. 48 (2013) 180–187.

[15] V.P. Raje, P.I. Morgado, M.P. Ribeiro, I.J. Correia, V.D.B. Bonifacio, P.S. Branco, et al., Dual on-off and off-on switchable oligoaziridine biosensor, Biosens. Bioelectron. 39 (2013) 64–69.

[16] B.K. Gorityala, Z. Lu, M.L. Leow, J. Ma, X.-W. Liu, Design of a "turn-off/turn-on" biosensor, J. Am. Chem. Soc. 134 (2012) 15229–32.

[17] X. Zhou, Q. Su, D. Xing, An electrochemiluminescent assay for high sensitive detection of mercury (II) based on isothermal rolling circular amplification., Anal. Chim. Acta. 713 (2012) 45–9.

[18] S. V. Wegner, A. Okesli, P. Chen, C. He, Design of an emission ratiometric biosensor from MerR family proteins: A sensitive and selective sensor for Hg2+, J. Am. Chem. Soc. 129 (2007) 3474–3475.

[19] Y. Yuan, M. Gao, G. Liu, Y. Chai, S. Wei, R. Yuan, Sensitive pseudobienzyme

Accepted manuscript

ACCEPTED MANUSCRIPT

electrocatalytic DNA biosensor for mercury(II) ion by using the autonomously assembled hemin/G-quadruplex DNAzyme nanowires for signal amplification., Anal. Chim. Acta. 811 (2014) 23–8.

[20] X. Cui, L. Zhu, J. Wu, Y. Hou, P. Wang, Z. Wang, et al., A fluorescent biosensor based on carbon dots-labeled oligodeoxyribonucleotide and graphene oxide for mercury (II) detection, Biosens. Bioelectron. 63 (2015) 506–512.

[21] J. Lee, H. Jun, J. Kim, Polydiacetylene-Liposome Microarrays for Selective and Sensitive Mercury(II) Detection, Adv. Mater. 21 (2009) 3674–3677.

[22] Y. Jiao, L. Zhang, P. Zhou, A rhodamine B-based fluorescent sensor toward highly selective mercury (II) ions detection, Talanta. 150 (2016) 14–19.

[23] A. Zahid, A. Lashin, U.A. Rana, N. Al-Arifi, I. Ullah, D.D. Dionysiou, et al., Development of surfactant based electrochemical sensor for the trace level detection of mercury, Electrochim. Acta. 190 (2016) 1007–1014.

[24] M.A. Armas, R. María-Hormigos, A. Cantalapiedra, M.J. Gismera, M.T. Sevilla, J.R. Procopio, Multiparametric optimization of a new high-sensitive and disposable mercury (II) electrochemical sensor, Anal. Chim. Acta. 904 (2016) 76–82.

[25] W. Abu Al-Soud, P. Rådström, Capacity of nine thermostable DNA polymerases to mediate DNA amplification in the presence of PCR-inhibiting samples, Appl. Environ. Microbiol. 64 (1998) 3748–3753.

[26] W.A. Al-Soud, L.J. Jönsson, P. Rådström, Identification and characterization of immunoglobulin G in blood as a major inhibitor of diagnostic PCR, J. Clin. Microbiol. 38 (2000) 345–350.

[27] I.G. Wilson, Inhibition and facilitation of nucleic acid amplification, Appl. Environ. Microbiol. 63 (1997) 3741–3751.

[28] E. Paspalakis, D.G. Angelakis, P.L. Knight, Influence of density of modes on dark lines in spontaneous emission, Opt. Commun. 172 (1999) 229–240. doi:10.1016/S0030-4018(99)00511-8.

Accepted manuscript

ACCEPTED MANUSCRIPT

[29] V. Yannopapas, E. Paspalakis, N. V. Vitanov, Plasmon-induced enhancement of quantum interference near metallic nanostructures, Phys. Rev. Lett. 103 (2009). doi:10.1103/PhysRevLett.103.063602.

[30] E. Paspalakis, C.H. Keitel, P.L. Knight, Fluorescence control through multiple interference mechanisms, Phys. Rev. A. 58 (1998) 4868.

[31] Q. Ge, Z. Liu, Y. Bai, D. Zhang, P. Yu, Z. Lu, Emulsion PCR-based method to detect Y chromosome microdeletions, Anal. Biochem. 367 (2007) 173–178.

[32] Z. Zhu, G. Jenkins, W. Zhang, M. Zhang, Z. Guan, C.J. Yang, Single-molecule emulsion PCR in microfluidic droplets, Anal. Bioanal. Chem. 403 (2012) 2127–2143.

[33] R. Williams, S.G. Peisajovich, O.J. Miller, S. Magdassi, D.S. Tawfik, A.D. Griffiths, Amplification of complex gene libraries by emulsion PCR., Nat. Methods. 3 (2006) 545–550.

[34] K. Shao, W. Ding, F. Wang, H. Li, D. Ma, H. Wang, Emulsion PCR: a high efficient way of PCR amplification of random DNA libraries in aptamer selection., PLoS One. 6 (2011) e24910.

[35] P. Corbisier, S. Bhat, L. Partis, V. Rui Dan Xie, K.R. Emslie, Absolute quantification of genetically modified MON810 maize (Zea mays L.) by digital polymerase chain reaction, Anal. Bioanal. Chem. 396 (2010) 2143–2150.

[36] T. Demeke, T. Gräfenhan, M. Holigroski, U. Fernando, J. Bamforth, S.J. Lee, Assessment of droplet digital PCR for absolute quantification of genetically engineered OXY235 canola and DP305423 soybean samples, Food Control. 46 (2014) 470–474.

[37] T.C. Dingle, R.H. Sedlak, C. Linda, K.R. Jerome, Tolerance of Droplet-Digital PCR vs Real-Time Quantitative PCR to Inhibitory Substances, Clin. Chem. 59 (2013) 1668–1669.

[38] D. Morisset, D. Štebih, M. Milavec, K. Gruden, J. Žel, Quantitative Analysis of Food and Feed Samples with Droplet Digital PCR, PLoS One. 8 (2013) e62583.

Accepted manuscript

ACCEPTED MANUSCRIPT

[39] M. Hori, H. Fukano, Y. Suzuki, Uniform amplification of multiple DNAs by emulsion PCR, Biochem. Biophys. Res. Commun. 352 (2007) 323–328.

[40] M. Nakano, Single-molecule PCR using water-in-oil emulsion, J. Biotechnol. 102 (2003) 117–124.

Accepted manuscript

Table 1 Elongation rates obtained using serial dilutions of the original Hg^{2+} solution

Final concentration of Hg^{2+}/ μmol L^{-1}	Amount of Hg^{2+}/ pmol	Elongation rate			Mean value	RSD of inner-group
5	100	39.565	41.284	38.603	39.817	2.785%
2.5	50	40.669	39.736	38.951	39.785	1.765%
2	40	38.726	40.782	35.505	38.338	5.665%
1	20	18.961	22.821	17.871	19.884	10.680%
0.5	10	10.187	11.421	8.920	10.176	10.034%
0.1	2	1.899	2.182	1.703	1.928	10.198%

ACCEPTED MANUSCRIPT

0.05	1	1.275	0.904	1.020	1.066	14.532%
0.02	0.4	0.226	0.499	0.433	0.386	30.130%
0.005	0.1	0.074	0.072	0.156	0.101	38.876%
0.002	0.04	0.050	0.071	0.031	0.051	32.244%
0.0005	0.01	0.003	0.005	0.006	0.005	26.726%
0.00025	0.005	0.001	0.000	0.003	0.001	
Negative	Negative	0.000	0.001	0.000	0.000	

Table 2 Measurements of environmental and clinical samples.

Sample type[1]	Hg^{2+} addition (molar amount added) / pmol	Qualitative results			Quantitative results/ pmol		
		1	2	3	1	2	3
Natural water	Negative[2]	-	-	-			
	2	+	+	+	2.201	2.121	1.913
	20	+	+	+	21.034	18.221	20.061
Serum	Negative	-	-	-			
	2	+	+	+	2.450	2.131	1.795
	20	+	+	+	21.081	19.421	20.909

1. The above table shows the quantitative and qualitative measurement results for the environmental and clinical samples. In this part of the experiment, both the negative sample and experimental sample with added Hg^{2+} were tested simultaneously.
2. The ICP-MS was taken to evaluate the content of Hg^{2+} within the original natural water. The final evaluation results were 0.05 ppb and 0.31 ppb for distilled water and natural water, respectively.

Figure Captions:

Figure 1 The mechanism of Hg^{2+} detection system based on mispairing biosensor and emulsion PCR

Figure 2 The secondary structure difference between biosensors with different T-Hg-T structures measured by circular dichroism.

Figure 3 The standard curve (a) and scatter diagram (b) between the content of Hg^{2+} and elongation rate

Accepted manuscript

ACCEPTED MANUSCRIPT

The equation and R^2 coefficient of the standard curve were listed in Figure 3a. The scatter diagram between the content and elongation rate was shown in Figure 3b, while the points of dynamic range were presented by triangle shape.

Figure 4 The evaluation of specificity of our Hg^{2+}detection system

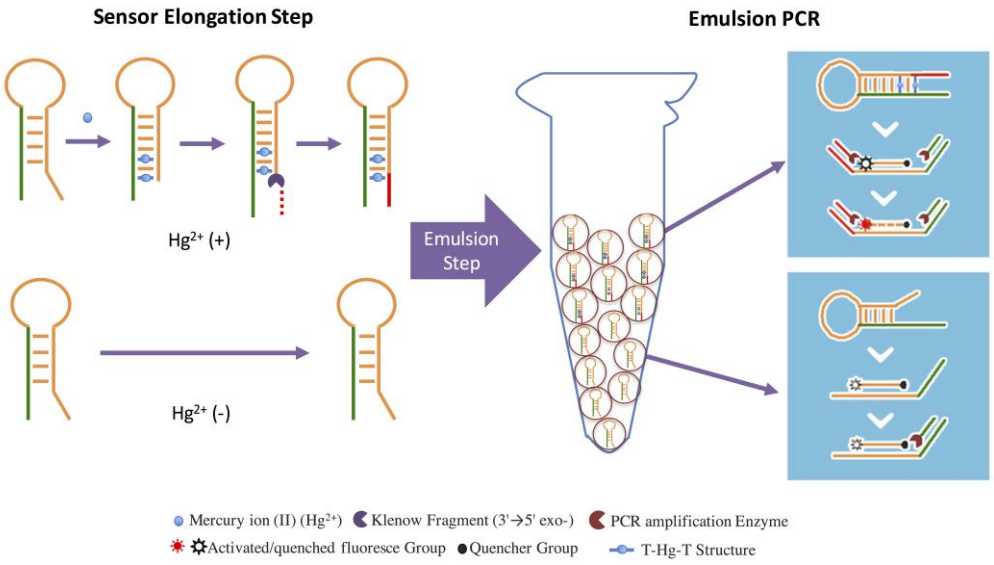

ACCEPTED MANUSCRIPT

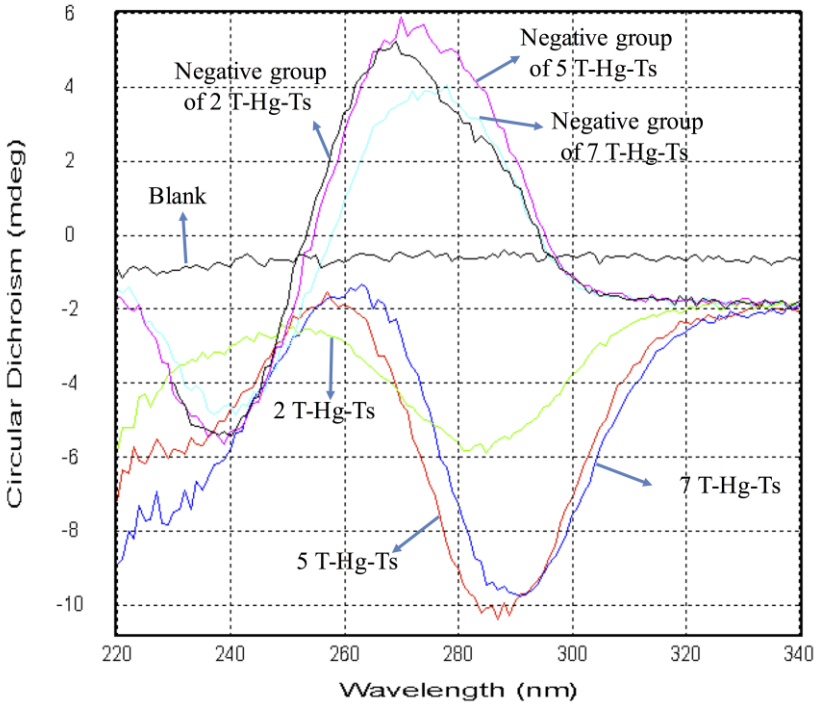

Accepted manu

ACCEPTED MANUSCRIPT

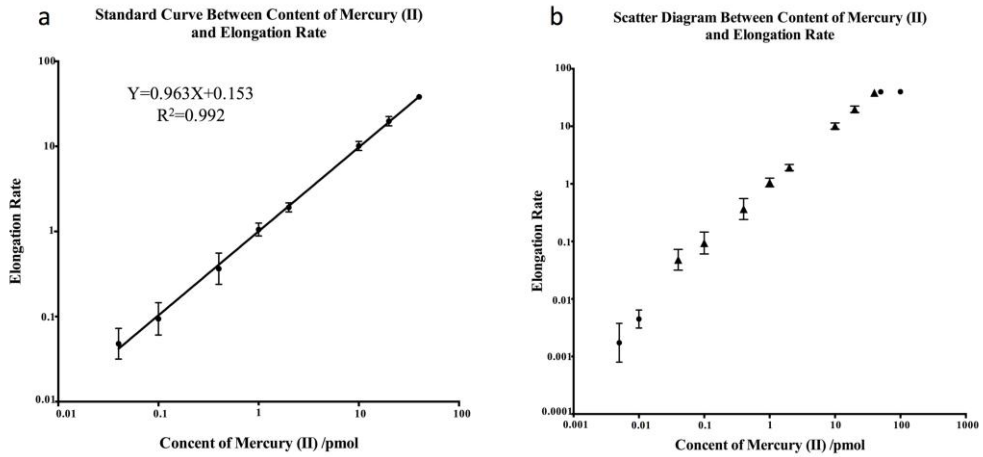

Accepted manu

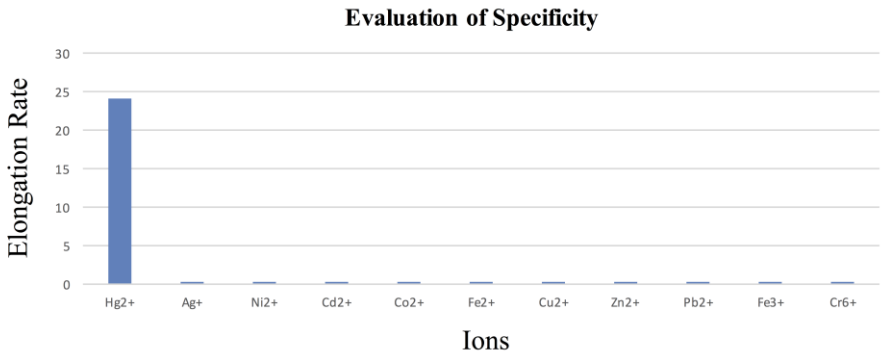

Accepted manu

Highlights

- Hg^{2+} detection system was revealed based on mispairing biosensor and emulsion PCR.
- It had a wide dynamic range from 40 pmol to 40 fmol over 4 logarithms.
- LOQ and LOD were set up as 40 and 10 fmol that could meet all detection demands.

Graphical abstract

ACCEPTED MANUSCRIPT

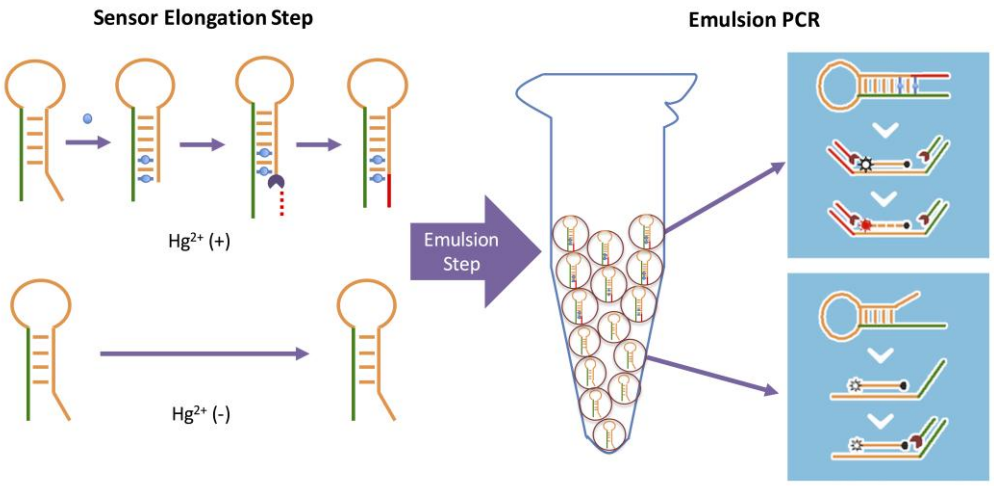

Accepted manuscript